SENSING ARRAY FOR COHERENCE ANALYSIS OF MODULATED AQUATIC CHEMICAL PLUMES

A Thesis
Presented to
The Academic Faculty

by

Ryan S. Cantor

In Partial Fulfillment
of the Requirements for the Degree
Master of Science in the
School of Chemistry and Biochemistry

Georgia Institute of Technology
May 2009

SENSING ARRAY FOR COHERENCE ANALYSIS OF MODULATED AQUATIC CHEMICAL PLUMES

Approved by:

Professor Jiri Janata, Advisor
School of Chemistry and Biochemistry
Georgia Institute of Technology

Professor Andrew Lyon
School of Chemistry and Biochemistry
Georgia Institute of Technology

Professor Marc Weissburg
School of Biology
Georgia Institute of Technology

Date Approved: April 1, 2009

To my family.

ACKNOWLEDGEMENTS

I thank Dr. Marc Weissburg and Dr. Don Webster for many helpful discussions and access to the flume facility. I also thank Dr. Mira Josowicz, Dr. George Yu, and Richard Bedell for their support designing and implementing submergible electrochemical sensors and the development of the supporting electronics. I would like to thank my advisor, Dr. Jiri Janata, for his continued support of my graduate education and my committee for reviewing this thesis. This work was supported by the NSF Signals in the Sea IGERT (Grant DGE 0114400) and the Georgia Research Alliance Eminent Scholar Fund.

TABLE OF CONTENTS

LIST OF TABLES

LIST OF FIGURES

SUMMARY

When a chemical is released from its source and disperses into the environment a chemical plume is formed as the released chemical mixes with the surrounding media. In a turbulent aquatic environment such as a flowing stream, this creates patches of relatively high chemical concentration surrounded by areas with lower concentrations.

Chemical plume tracking relies on converting downstream chemical signals into navigational cues. Some methods evaluate chemical signals in the time domain. However, when a modulation frequency is superimposed onto the random patchiness observed in turbulent plume, analysis in the frequency domain can provide additional navigational information. Modulated plumes can be generated manually by controlling the release of the chemical signal or more naturally as chemical plumes interact with objects in their path.

The goal of this work was to demonstrate the extraction of frequency encoded information from modulated aquatic chemical plume using an array of electrochemical sensors. Coherence analysis provides a useful tool to correlate the chemical signals detected from spatially separated sensors in the array.

Model systems initially were investigated to assess the feasibility of applying coherence analysis to chemical plume tracking. First, an optical method, planar laser induced fluorescence (PLIF), was used to generate data sets for the time varying concentrations in a single plane of the plume. By analyzing specific points in this plane, sensor configuration and placement was investigated. Next, a bench top fluidic system was used to deliver chemical signals to an amperometric sensor array. The bench top system generated defined chemical signals with features that simulated turbulent

plumes and allowed the development and optimization of the electrochemical sensors.

Finally, an electrochemical array was developed to evaluate real modulated chemical plumes. Several technical hurdles were overcome, such as designing submergible sensors, building a multipotentiostat to detect the chemical signals from a sensor array, and customizing data acquisition and analysis. After developing the experimental setup, coherence analysis was applied to extract the frequency components contained in modulated turbulent plumes. Effects due to release distance, modulation frequency, and array orientation were investigated.

This work was published in the paper "Sensing array for coherence analysis of modulated aquatic chemical plumes", Cantor, R.S.; Ishida, H.; Janata, J.; Analytical Chemistry 2008, 80, 1012-1018.

CHAPTER I

INTRODUCTION

1.1 Chemical Plume Tracking

Animals commonly rely on chemical signals as they search for resources (food, mates, etc.) and avoid danger (predators, competitors, etc.). Robots also rely on chemical signals as they search for the source of a chemical release. A chemical plume is created when chemical signals emanate from a source and travel through the surrounding environment a chemical plume is created (Figure 1).

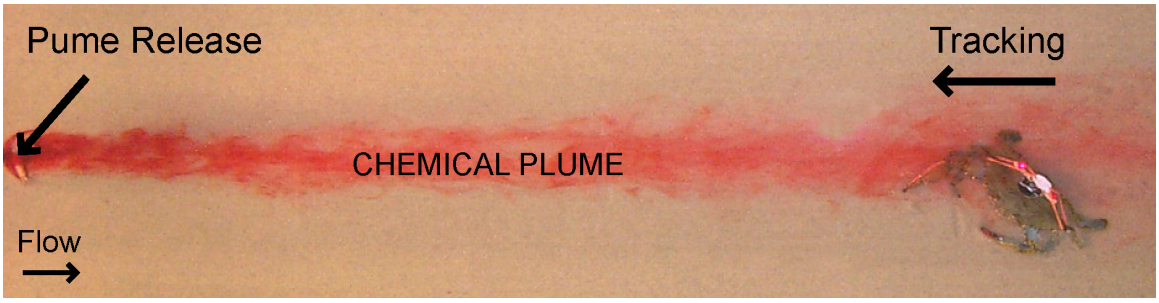

Figure 1: A blue crab tracking toward the source of an aquatic chemical plume

Chemical plume tracking requires the acquisition and processing of chemical and spatial information downstream from the source of chemical release and determination of navigation cues that direct movement towards the source. Experimental testing of aquatic navigational strategies is an inherently multidisciplinary field with both biological and engineering importance [1]. Chemists have created aquatic chemical sensors [2]. Biologists have studied the way animals navigate toward odor plumes [3]. Engineers have built plume tracking robots [4]. Understanding of the physics governing plume structure has been a focus of fluid mechanics [5].

As a chemical marker is transported from its source in a turbulent environment,

instantaneous concentrations downstream can be expressed as the sum of mean concentration and a fluctuating concentration. The detected signal (e.g. fluorescence, electrochemical, conductivity) is a function of concentration, mass transport of the chemical marker, and a proportionality constant determined by the sensing principle. These signals are further influenced by obstacles placed in their path. Objects introduce turbulence and add additional fluctuations in marker concentrations. Thus an odor plume can be pictured as fluctuating chemical signal based on the source, turbulent mixing, diffusion, and any obstacles it has passed over. A plume not only holds chemical information about the source identity but its creation and transport encode information about the source shape, location, and the environment it has traveled through [6, 7].

Chemical release and transport in a turbulent medium determines the fine-scale structure of the resulting patchy meandering plume. The spatial structure can be perceived as temporal fluctuations of a chemical signal by a sensor placed at a fixed position in the plume. The structure of the plume, its information content, and the signal processing algorithms needed to characterize it can be studied using chemical markers [6, 7, 8, 9, 10]. A simple navigational strategy involves the detection of the time averaged signal in order to recognize concentration gradients in the long term steady state signal. However, there are several inherent difficulties including increased measurement time, baseline stability, and sensitivity [5]. For real time plume tracking, more instantaneous parameters are typically used. Various properties of a signal, such as intermittency and the rising slope of bursts, have been studied with respect to their dependence on the distance from the source [6, 7].

1.2 Modulated Chemical Plumes

In addition to the inherent random signal fluctuation in turbulent plumes, natural phenomenon can create plumes with specific modulation frequencies. For instance, in

the certain conditions, when a continuous chemical plume passes around a bluff body obstacle, the shedding of alternating eddies creates a discrete modulation frequency in the downstream chemical plume structure. It has been hypothesized that information about the position of the source could be encoded in the frequency domain of the chemical signal.

A simple way to encode specific modulation frequencies into a plume is the controlled release of a chemical marker solution. A pulse modulated plume can be generated using a solenoid valve to control the release of solution thereby allowing direct control of the pulse size of and frequency of modulation.

Alternatively, objects placed in the direct path of a continuous (unmodulated) plume can impart a modulation frequency as observed in the formation of a vortex street. Fluid flow around an obstacle creates a wake pattern of alternately shed vortices. In the case of a cylinder, a von Kármán vortex street is formed with a dominating shedding frequency, f_s, which can be calculated using $f_s = St(V/D)$ [11]. The shedding frequency is a function of the stream flow velocity, V, and cylinder diameter, D, and normalized to the Strouhal number, St. The Strouhal number has a numerical value of approximately 0.2 over a wide range of Reynolds numbers, including the turbulent environment used in these experiments. The shape of the object also affects the frequency of modulation and the downstream plume shape. A variety of cylinder and cube obstructions have been studied [12, 13].

1.3 Passive vs. Active Plume Characterization

In this work, several methods were used to study modulated plumes. Turbulent plumes were created by releasing chemical markers into an aquatic flume. Detection of the chemical marker was achieved passively through optical sensing by a remote detector (CCD camera) and directly by an electrochemical sensor array placed in the plume. Additionally, a bench top fluidics system was used to simulate features of a

turbulent plume in order characterize electrochemical sensor array response.

Planar laser induced florescence (PLIF) is a nonintrusive, optical measurement technique used to obtain a sequence of instantaneous, high-resolution spatial concentration fields. Each pixel can be considered a virtual sensor, and large areas of the flume can be sampled simultaneously. Typically, PLIF data is constrained to a single plane of the flume on which the light sheet is shed, although methods have been developed to probe the three-dimensional space of the plume by rastering the horizontal plane in the vertical direction [14]. PLIF is a valuable for probing large areas of the flume and characterizing plumes.

Detecting chemical plumes directly with real physical sensors (contact sensors) provides a more "real world" picture of the challenges in accurately tracking chemical plumes. Contact sensors have the ability to sample specific points in the plume in three dimensional arrangements at high sample rates. However, size and shape of the sensor, response time, and sensitivity all have an effect on signal structure and can introduce noise. Additionally, a limited number of discrete sensors can be included in the array. A major advantage of contact sensors are their suitability for implementation in robotic tracking systems. Electrochemical sensors are a natural choice because they directly convert the chemical signal to an electrical signal. Amperometric sensors are attractive due to their fast response times. Contact sensors can create disturbances in the plume structure because of their physical presence. This allows insight into the types of signal structure changes due to physical bodies deforming the flow that may be experienced by animals tracking toward a plume.

1.4 Project Goals

The primary goal of this work was the development and application of a contact sensor array system capable of detecting modulated chemical plumes in a turbulent flume environment. PLIF data was used to demonstrate the feasibility of encoding and

extracting the modulation frequency from an object modulated chemical plume. In order to develop suitable chemical sensors and data evaluation methods a bench top fluidic system was used to simulate chemical plume signals [15]. Finally a sensor array system was developed to detect directly both pulse modulated and object modulated plumes in the turbulent environment experienced in an aquatic flume.

CHAPTER II

EXPERIMENTAL METHODS

2.1 Bench Top Fluidic System

The goal of the bench top fluidic system experiments was to explicitly demonstrate an improved signal-to-noise ratio when using a sensor array to detect modulated chemical signals. The experimental setup has been previously described [15, 16]. Briefly, the bench top fluidic system is similar to flow injection analysis and delivers carrier solution (0.5M NaCl) through tubing delay elements (0.5 mm i.d.). The stream is divided into four channels each containing an amperometric sensor housed in a flow-through cell. An electroactive marker (ascorbic acid solution) is delivered into the carrier stream as a series of concentration pulses at the modulation frequency, 1 Hz.

2.2 Detecting Modulated Chemical Plumes in an Aquatic Flume System

Coherence analysis of chemical plumes generated in an aquatic flume system were conducted. In separate experiments, both PLIF and electrochemical measurements were made. The goal of the PLIF experiments was to use virtual sensors to determine the array distances and orientations suitable for the extraction of the modulation frequencies with coherence analysis. The goal of the electrochemical experiments was to demonstrate the extraction of modulation frequency with an electrochemical sensor array and to determine the orientation of the array with respect to the plume using the detected modulation frequency.

2.2.1 Generating Modulated Chemical Plumes

Modulated chemical plumes were generated in the flume system. Uniform flow with constant average velocity (3.0, 4.0, or 5.0 cm/s depending on the experiment) and water depth of 20.0 cm was established in a 1.07 m wide, 24.4 m long recirculating freshwater flume with sand covering the flume floor.

A chemical plume was formed by releasing a chemical marker solution from a release nozzle (4 mm i.d.) positioned on the flume centerline, into the fully developed boundary layer of the open channel flow. The chemical marker chosen was dependent on the data collection method employed, and the release rate was controlled using a micrometering valve and rotometer. The effluent velocity was matched with the channel flow velocity thus creating a passive source and avoiding the production of additional turbulence by shear induced by the effluent. For pulse modulation of the plume, the solution was released at a specific frequency governed by a three way computer controlled solenoid valve. This method provided very discrete packets and allowed easy adjustment of the modulation frequency to determine the bandwidth of the analysis. For object modulation of the plume, a vertical cylinder with a diameter of 0.8 cm was placed 2.5 cm downstream of a continuous marker solution release.

2.2.2 PLIF Data Collection

Planar laser-induced fluorescence (PLIF) was used to collect chemical data optically from modulated chemical plumes. The details of the experimental setup have been previously described [5]. A dilute fluorescent dye, rhodamine 6G, was used as the chemical marker. An argon-ion laser beam in a plane parallel to the bed with a scanning mirror created the illumination sheet at the same height above the flume bed as the plume release (2.5 cm). The laser light caused the dye to fluoresce, and a digital CCD camera captured the emitted light. The light intensity emitted by the dye is directly proportional to the dye concentration. Extracting the fluorescent

intensity from a specific location in the plane generates the concentration response of a virtual sensor at that location. Data was collected at 10 Hz for 10 minutes. Smaller portions of this time record were used in the analysis. The response of an array of seven virtual sensors was extracted at varying downstream distances from the plume release and at varying angular orientations to the plume centerline.

2.2.3 Electrochemical Data Collection

In a second set of experiments, an array of contact sensors was used to collect electrochemical measurements from modulated plumes. Ascorbic acid (50 mM) was used as the chemical marker. The release nozzle was positioned on the flume centerline and at an 11 cm height above the flume substrate to counteract the sinking nature of the marker solution.

A sensor array consisting of seven working electrodes (disk electrodes, 300 μm graphite sealed in 2 mm glass) was placed downstream from the release nozzle. Graphite electrodes proved suitable due to their ease of fabrication, ruggedness, fast reproducible responses, and minimal fouling during the course of the experiment. A counter electrode (steel rod) and the reference electrode (Ag/AgCl in 1 M KCl) were placed close to the array. A lab built multichannel potentiostat was used to apply 600 mV between each working electrode and a common auxiliary electrode and monitor the current response due to the oxidation of ascorbic acid. The potentiostat system and wiring was shielded to remove environmental noise experienced in the hydraulics lab housing the flumes. A data acquisition card (National Instruments) with Labview software was used to collect data from the potentiostat.

2.3 Data Processing and Coherence Analysis

Data were analyzed using the Matlab software package (The MathWorks, Signal Processing Toolbox). First, the raw sensor responses were summed to 10 samples/s. To remove low power but very coherent noise in the system, response data with a

value less than a threshold ($\sim$ 10 x baseline) was set to 0. Decoding the modulation frequency from the sensor response is most robustly observed through coherence analysis. The coherence parameter, $\alpha(\omega)^2$, measures the normalized energy in the common signal between two spatially separated sensors at a given frequency range.

$$\alpha(\omega)^2 = \frac{\mid X_{jk}(\omega) \mid^2}{\mid X_{jj}(\omega) \mid\mid X_{kk}(\omega) \mid}$$

Coherence of the signals from two sensors (j and k) is the ratio of their power spectral densities ($X_{jj}(\omega)$ and $X_{kk}(\omega)$) and their cross power spectral density ($X_{jk}(\omega)$). Coherence is a function of frequency varying from 0 for completely uncorrelated signals to 1 for completely correlated signals. A more detailed description of this analysis is presented in our previous work [15, 16, 17, 18].

A background data set was collected to confirm that signals observed in the electrochemical detection were truly caused by chemical plume modulation. Both a continuous release of 50 mM ascorbic acid and a pulsed blank release of flume water showed no specific low-frequency coherence signals. However, pulsed releases of ascorbic acid solutions yielded the expected coherence signals at the modulation frequencies.

When more than two sensors were considered, an averaged coherence spectrum for the set was calculated by averaging the spectra obtained from every unique pairing of those specific sensors. For each averaged coherence spectrum, the normalized modulation signal strength was calculated by dividing the intensity of the peak in the averaged coherence spectrum at the pulse frequency by the baseline (median of the specific spectrum). Plotting normalized modulation signal strengths allowed clear comparison of varying sensor selections, pulse frequencies, and release distances.

CHAPTER III

RESULTS

3.1 PLIF Results

3.1.1 Distance and Orientation Effects on Decoding an Object Modulated Plume

Coherence analysis of PLIF data was used to determine the approximate distance that the plume maintains a modulated structure and to determine the effects of array positioning and angle on the detection of modulation frequency. Coherence spectra were calculated for a sensor array configuration at different distance positions and orientation angles in the plume (Figure 2). For each position, 30 s data segments were extracted for the seven virtual sensors in the array. The coherence spectra for each unique pair (21 pairs) were averaged together yielding the averaged coherence of the array at that position.

For the case of a cylinder modulating a plume at 1 Hz, the modulation peak detected at 1 Hz decayed as the distance between the array and the cylinder increased. The modulation was undetectable at a distance of 8 cm or more, which is consistent with the visual inspection of the collapse of the vortex street structure.

The angle dependence of the coherence spectrum suggests that the transverse arrangement (i.e., 0°) of the sensors is the best for effective data collection. In contrast, when the array is oriented parallel to the flow direction (i.e., 90°), the coherence spectra reveal correlated signal at all frequencies and, therefore, the small modulation peak was buried in the "noise". Nevertheless, this orientation may provide useful information about the average flow velocity based on the time delay of individual filaments arriving at consecutively positioned virtual sensors. This orientation would not yield suitable signals with contact sensors because of plume structure deformation

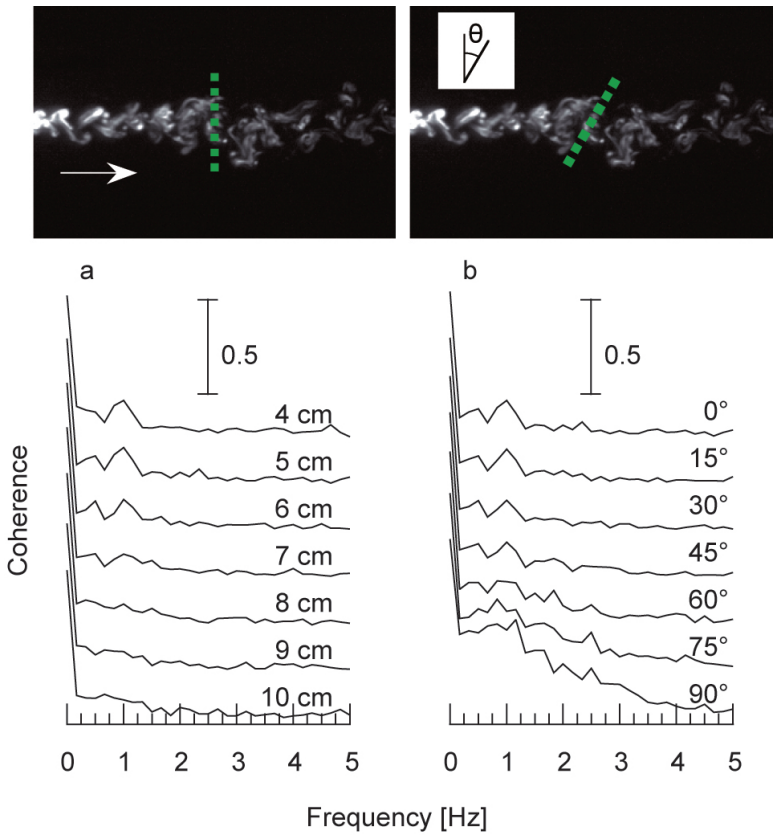

Figure 2: Array distance and orientation effects on averaged coherence: The sensor array's averaged coherence was calculated from the PLIF concentration fields for specific array distances and angular orientations. The spacing of individual sensing elements is not to scale in the images. (a) Changes in the coherence spectra when the array is moved along the centerline of the plume between 4 and 10 cm from the cylinder. (b) Variation of the coherence spectra due to the array orientation. For each orientation, the center of the sensor array is located at 5 cm from the cylinder. $\theta = 0°$ corresponds to transversely oriented array elements as in part a.

from the sensor bodies.

3.2 Bench Top System Results

3.2.1 Increasing Signal to Noise Ratio with a Sensor Array

An important consideration when extracting embedded signals is the time length of the record required to resolve the information. When a single pair of sensors is analyzed using coherence analysis, long time records are required distinguish the modulation frequency peak due to the random turbulent chemical signals obtained by

a single pair of sensors. The bench top virtual plume system was used to determine if increasing the number of sensors increases signal strength in a shorter time series (Figure 3a). The coherence spectrum obtained with a 1000 s time series from one pair of sensors has a clear peak at the modulation frequency, f_0, and at its higher harmonics (2, 3, and 4 Hz) (Figure 3a curve i). Coherence estimated from insufficiently long records (50 s) from the virtual plume contains large variation (Figure 3a curve ii). Increasing the number of sensors in the array and evaluating the commonality between different sensor pairs can shorten the acquisition time necessary to clearly observe the modulation frequency. The signal to noise ratio for the modulation frequency is significantly improved by increasing the number of channels to four and averaging the coherence spectra from the six possible sensor pairs (1-2, 1-3, 1-4, 2-3, 2-4, and 3-4). The strength and frequency of the false peaks in the coherence estimation differ among various pair selections. Therefore, averaging the coherence spectra for multiple sensor pairs significantly smooth the spectra (Figure 3a curve iii).

3.2.2 Increasing Modulation Signal Detection with Array Tuning

When the modulation frequency is known a priori, the quality of the coherence spectra can be further improved by tuning the array to that specific frequency. PLIF data was used to demonstrate increased signal strength by selecting specific sensors (Figure 3b). With 7 sensors, a total of 21 unique pairs can be formed to calculate the coherence function (Figure 3b curve i). Since the extent of frequency modulation differs at different locations within the plume, some pairs show a large peak at the 1 Hz modulation frequency (Figure 3b curve iii) and some show no peak at the same frequency (Figure 3b curves iv and v). Selecting the pairs with large coherence values at 1 Hz and discarding the other coherence pairs "tunes" the array to that frequency (Figure 3b curve ii). This form of tuning is appropriate when sensing in the wake of an object of a known size or a chemical release pulsing at a known frequency. It was

found that sensors showing the highest modulation frequency signal were those positioned in the centermost part of the plume. The sensor pairs containing sensors at the fringe of the plume show only nonspecific noise. Therefore averaging in-plume sensors provided a guide for tuning the contact sensor arrays in the following experiments.

3.3 Contact Sensor Array Results

3.3.1 Determining In-Plume and Out-of-Plume Contact Sensors for Coherence Analysis

In order to test the ability of coherence analysis to distinguish in-plume and out-of-plume sensors, the arrays positioning in the plume was first determined by analyzing the time series response and the power spectral density of each sensor.

Two contact sensor array configurations were investigated. First, a linear array was used to gather information in one dimension on the horizontal plane of the flume (Figure 4a). Then, a planar array was used to gather information in two dimensions on the vertical plane of the plume (Figure 4b). In both arrays, sensors were spaced 5 mm (center to center) from each other and the array center (sensor 4) was positioned 10 cm above the bed on the plume centerline. The relative position of array in the plume is evident in the time series response to a 1 Hz pulse modulated plume (Figure 5). By averaging the sensor response over the entire time series, the sensors showing the greatest response to the ascorbic acid indicates where the plume is centered in the array (Figure 4c). The approximate symmetrical distribution of responses also confirmed that the array was centered on the plume. Power spectral density analysis of the individual sensors response showed much higher baseline spectral power for sensors in the plume and was used as a complementary method for verifying in-plume sensors.

The total averaged coherence value for the array was calculated by averaging the coherence spectra calculated for every unique combination of the sensors. In-plume averaged coherence and out-of-plume averaged coherence were calculated by only

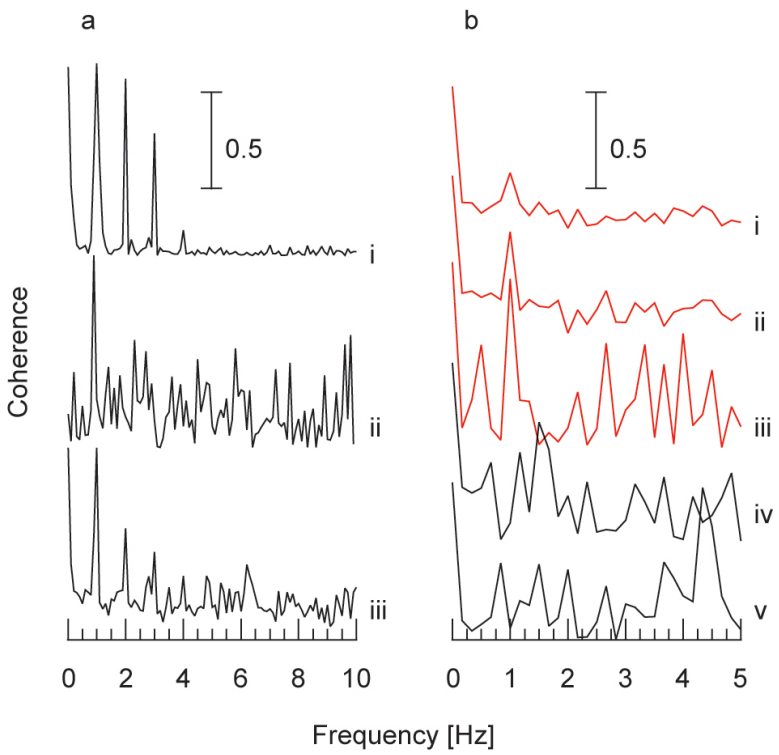

Figure 3: Array size and tuning effects on modulation frequency detection: (a) Signals obtained with a four channel electrochemical sensing array in the bench top fluidic system. The coherence spectrum obtained from (i) 1000 s time series from two sensors (one pair), (ii) 50 s time series from two sensors (one pair). (iii) 50 s time series from four sensors (six unique pairs). (b) Coherence spectra calculated from 30 s PLIF records similar to those shown in Figure 1a. (i) The average of coherence spectra for all 21 possible pairs. (ii) Tuning the response to a fixed frequency by selecting and averaging only the pairs with the 10 highest values of coherence at the target frequency. Parts iii, iv, and v are the nonaveraged coherence spectra of sensor pairs 3-5, 5-7, and 1-4, respectively. The "inner" sensor pair, 3-5, shows a distinctly high value at f_0 but also a high nonspecific noise at higher frequencies. The sensor pairs containing sensors at the fringe of the plume (1 and 7) show only nonspecific noise.

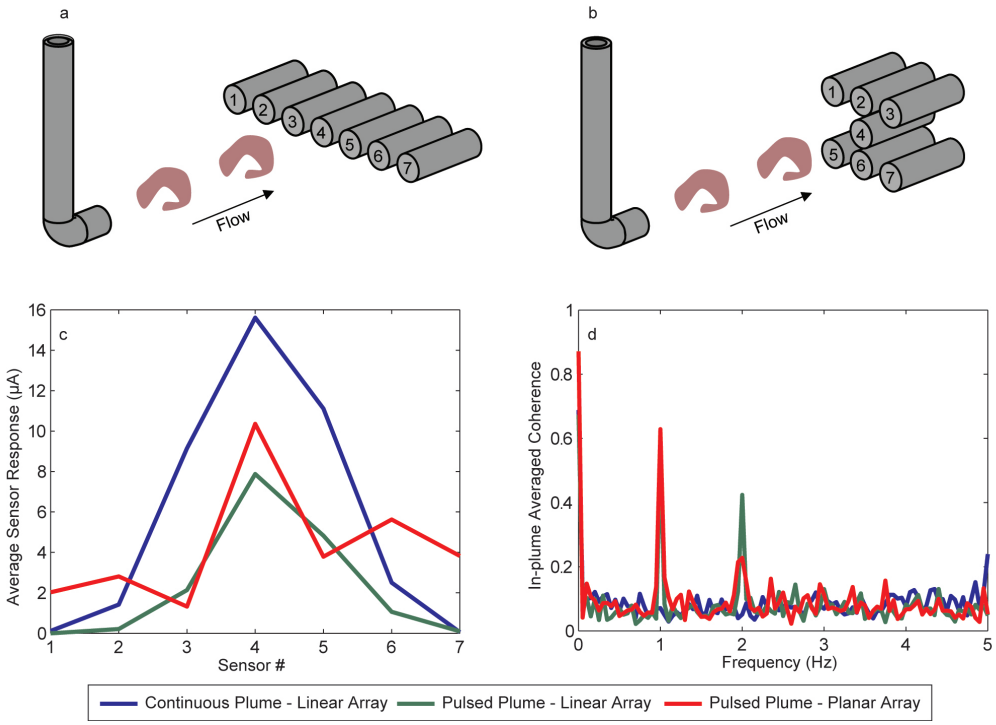

Figure 4: Modulated plume detection by linear and planar arrays: (a) linear and (b) planar contact sensor arrays were placed in a 1 Hz pulse modulated ascorbic acid plume. In both cases, the array height is 10 cm above the flume substrate and the release distance is 5 cm. Time series were collected for 300 s for each configuration. (c) To verify the array orientation with respect to the plume, average sensor response over the entire time series was calculated. Response from a continuous plume release is shown for comparison. (d) Coherence analysis of the strongest responding sensors (in-plume) for each configuration shows peaks at the fundamental modulation frequency and its first harmonic.

averaging the unique pairs of the set of sensors identified as either in the plume or out of the plume. When a pulse modulated plume was delivered to both the linear and planar contact sensor array configurations, a clear peak is observed in the coherence spectra at the modulation frequency (1 Hz) and its first harmonic (2 Hz) (Figure 4d). A continuous plume (not modulated) does not show a peak in the coherence spectrum.

3.3.2 Observing Array Orientation through Contact Sensor Array Tuning

The PLIF experiments indicated that sensors centered on the plume contain the strongest modulation frequency signals. For the contact sensor experiments, groups

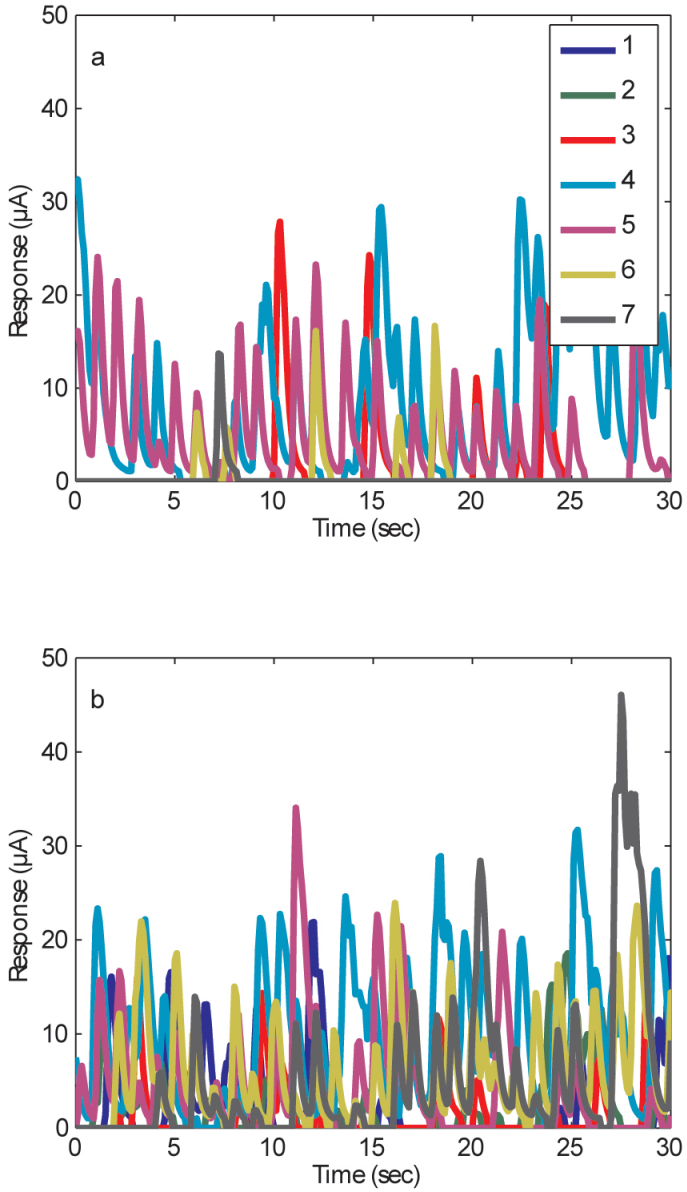

Figure 5: Typical time series data collected from a linear array (a) and a planar array (b) positioned in a 1 Hz pulsed ascorbic acid plume. In both cases the array height is 10 cm above the flume substrate and the release distance is 5 cm. Segments of the 300 s time series collected are shown for each configuration after integrating for 10 samples / second and applying a response threshold of 1 μA current. Each line corresponds to an individual sensor response.

of sensors were defined by the array orientation in the plume. For the linear array, total, in-plume, and out-of-plume sensor selections were considered. For the planar array, total, top, bottom, right, middle, and left sensor selections were considered. The averaged coherence spectra were calculated for each sensor grouping (Figure 6 to 9). Coherence analysis of these specific groups of sensors shows the relationship of the array position to the most modulated part of the plume and determines the relative bias in the signal based on the sensor group's position.

The total averaged coherence spectrum showed the lowest baseline due to the inclusion of out-of-plume sensors that carry minimal signal. Only the in-plume sensors carry the modulation signal, so selecting in-plume sensors for averaging shows a substantial increase in the normalized modulation signal strength compared to the out-of-plume or total sensor sets. In the linear array cases (Figures 10 and 11), the array is centered on the plume and the middle sensors (in-plume) carry the signal. If the array was positioned off center the lateral bias would be observed by a stronger signal from the right or left sensors.

The planar array is capable of extracting both lateral and depth bias information. A strong signal increase is found when selecting the bottom sensors (Figures 12 and 13) indicative of the plume contacting the bottom most sensors due to sinking of the slightly denser ascorbic acid solution. Symmetry in the lateral array position is observed as no clear signal strength improvement from selecting right or left sensors (Figures 12 and 13).

3.3.3 Effects of the Pulse Frequency and Release Distance

Averaged coherence analysis of in-plume sensors allows the detection of pulse frequencies up to to $\sim$2.5 Hz (Figures 10 and 12).The pulses become smaller and closer together as the pulse frequency gets higher; therefore, turbulent mixing has a greater effect in causing the chemical packets to overlap.

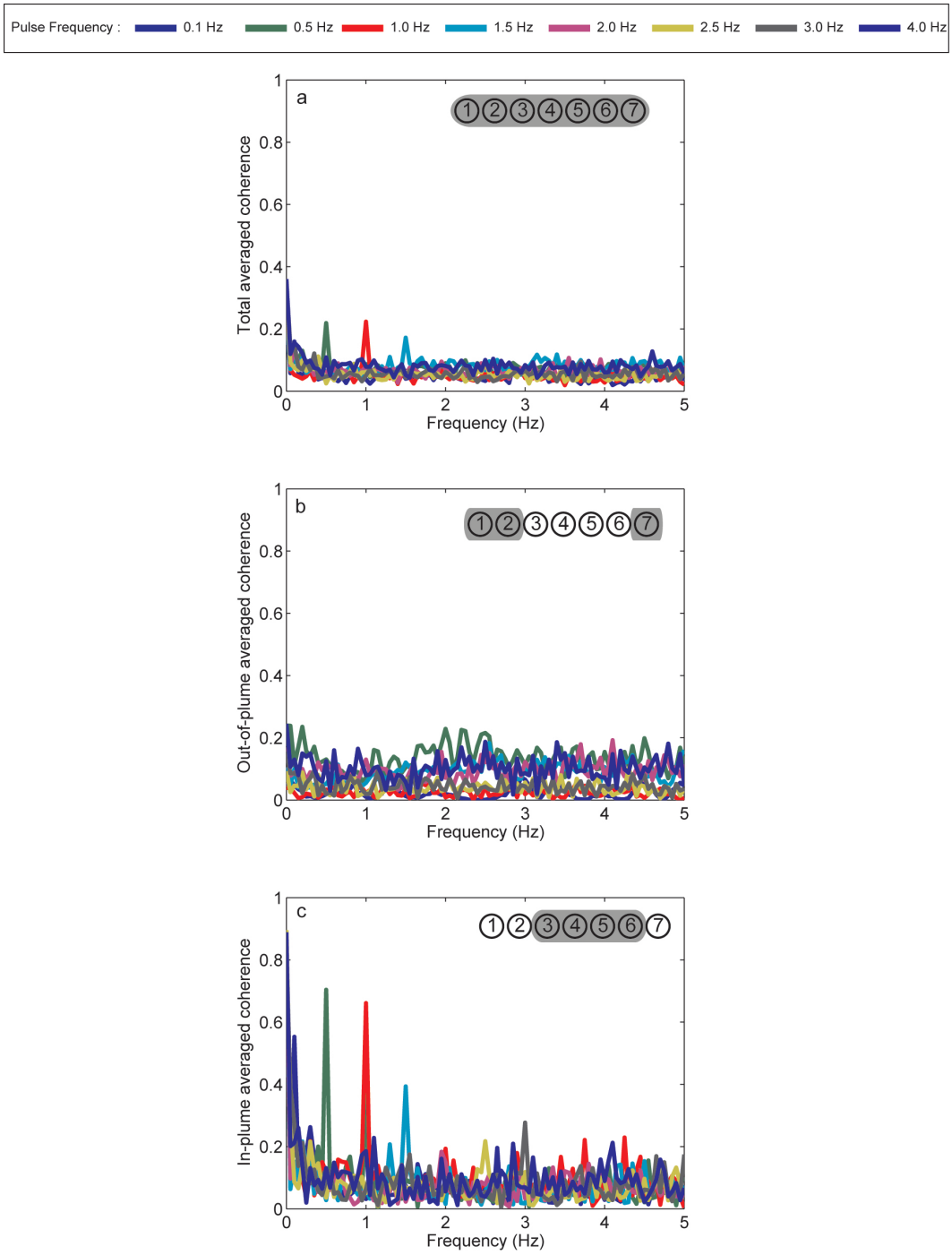

Figure 6: Coherence Spectra from a Linear Contact Array Varying the Pulse Frequency. A solenoid valve was used to deliver a modulated plume at varying pulse frequencies to a linear sensor array (7 sensors 5 mm spacing) with a 5 cm release distance (Figure 4a). Data was collected at each frequency for 300 s. Coherence spectra were averaged for of all of the sensors (a), sensors outside of the plume (b), and sensors inside of the plume (c).

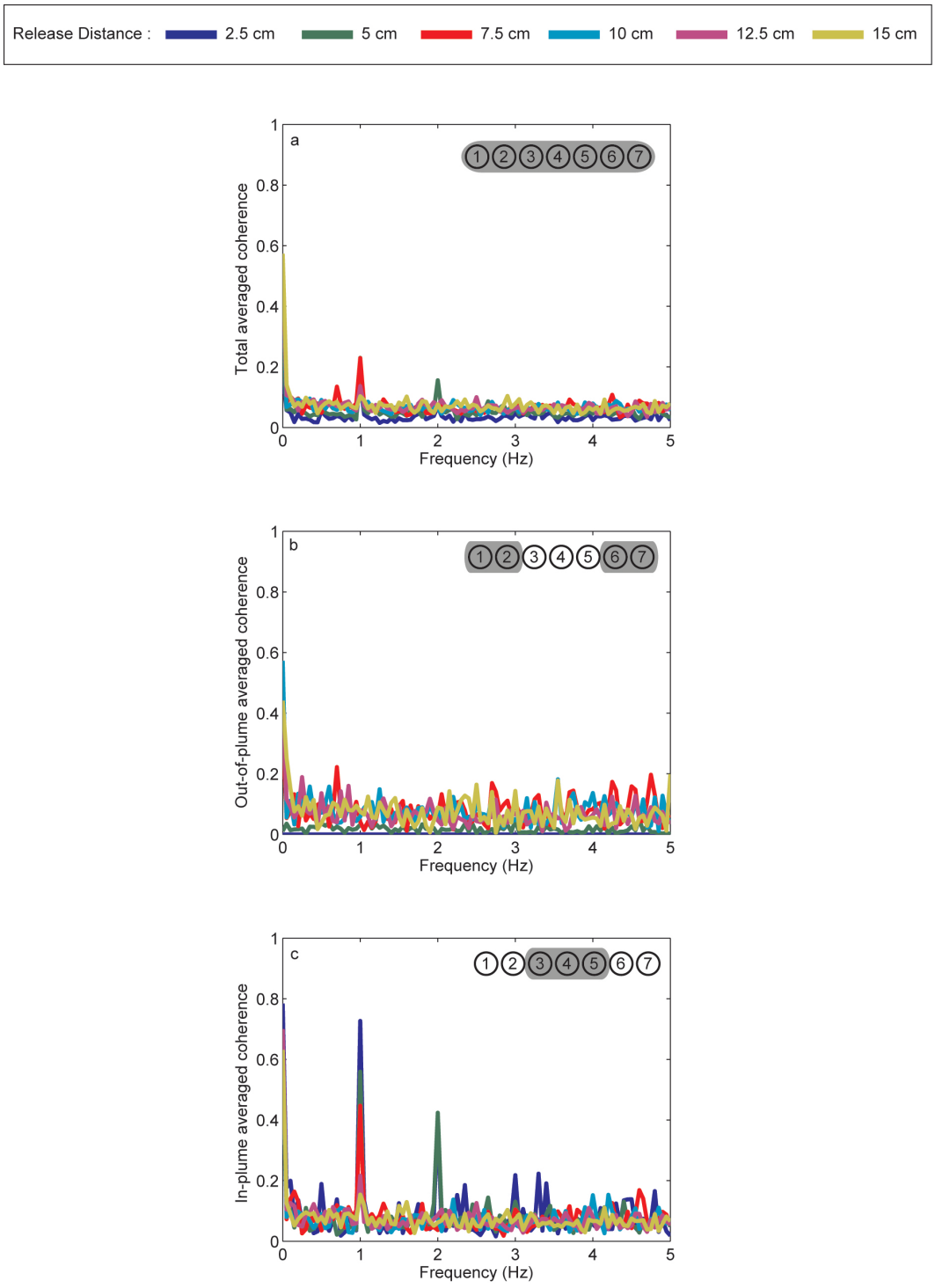

Figure 7: Coherence Spectra from a Linear Contact Array Varying the Release Distance. A solenoid valve was used to deliver a modulated plume (1 Hz) to a linear sensor array (7 sensors 5 mm spacing) with varying release distances (Figure 4a). Data was collected at each distance for 300 s. Coherence spectra were averaged for of all of the sensors (a), sensors outside of the plume (b), and sensors inside of the plume (c).

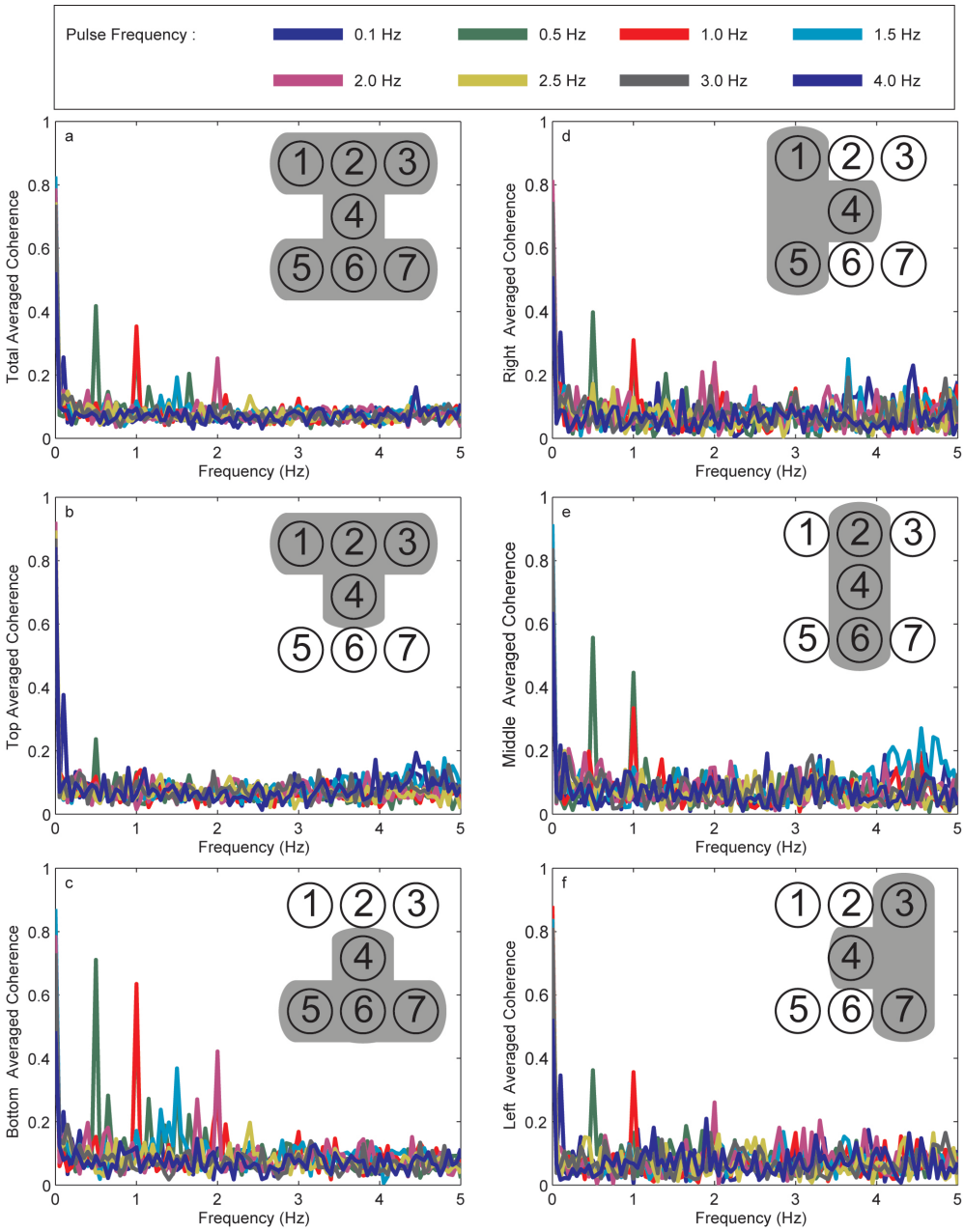

Figure 8: Coherence Spectra from a Planar Contact Array Varying the Pulse Frequency. A solenoid valve was used to deliver a modulated plume at varying pulse frequencies to a planar sensor array (7 sensors 5 mm spacing) with a 5 cm release distance (Figure 4b). Data was collected at each frequency for 300 s. Coherence spectra were averaged for of all of the sensors (a), top sensors (b), bottom sensors (c), right sensors (d), middle sensors (e) and left sensors (f).

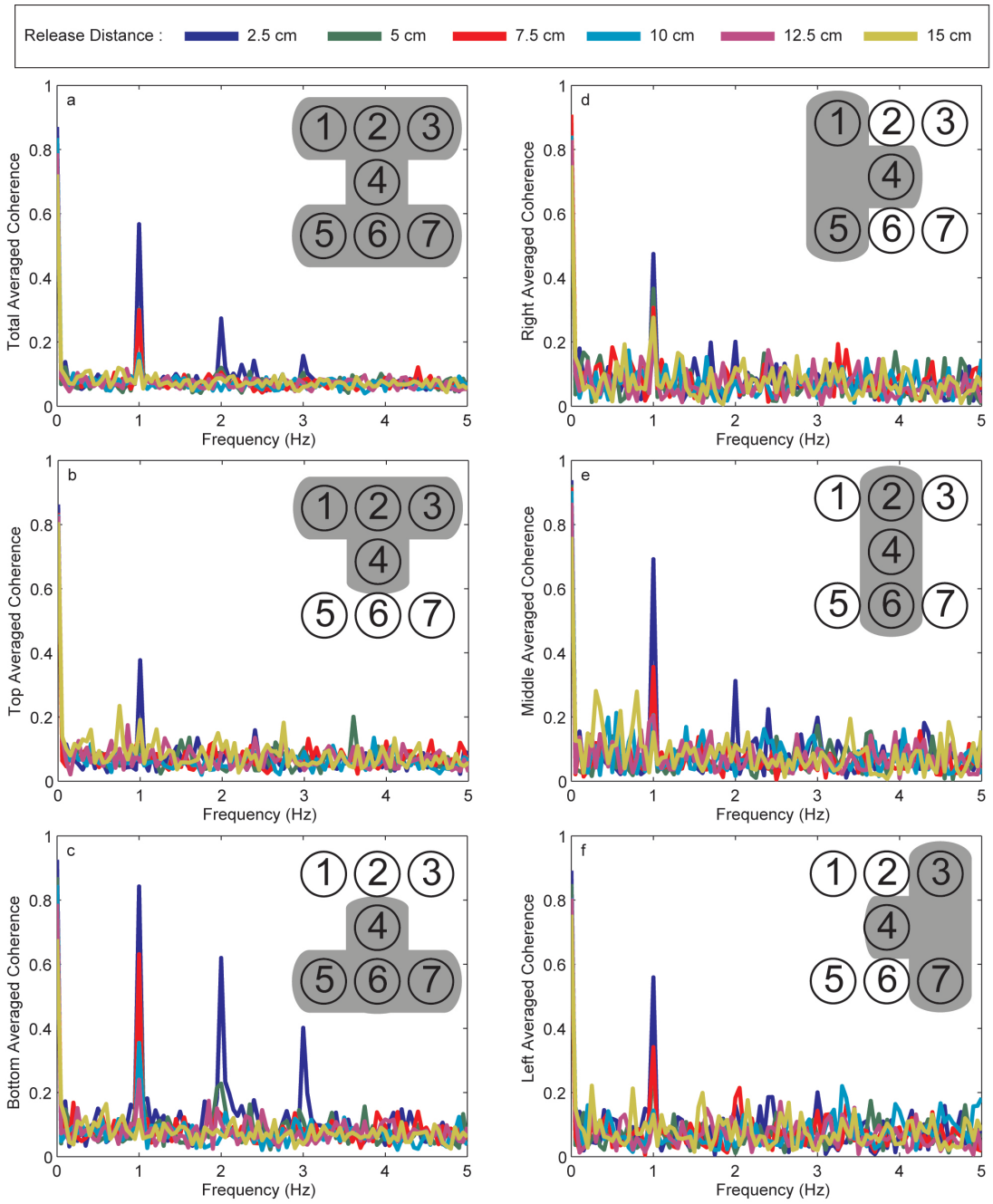

Figure 9: Coherence Spectra from a Planar Contact Array Varying the Release Distance. A solenoid valve was used to deliver a modulated plume (1 Hz) to a planar sensor array (7 sensors 5 mm spacing) with varying release distance (Figure 4b). Data was collected at each distance for 300 s. Coherence spectra were averaged for of all of the sensors (a), top sensors (b), bottom sensors (c), right sensors (d), middle sensors (e) and left sensors (f).

A 1 Hz pulse frequency (Figures 11 and 13) was detectable at release distances of up to to ∼13 cm. Increasing the release distance allows more mixing of plume causing decreasing the chemical signal peak height and the sharpness of pulses. Also, at greater release distances the trail of pulsed packets meanders, periodically contacting different sensors in the array. Chemical packets are spaced at distances governed by the modulation frequency. However, the probability of every packet hitting the same set of sensors decreases with the increased release distance. Both of these effects cause a decrease in coherence signal.

Release distance affects the occurrence of harmonic signals in the coherence spectra of in-plume sensors. At very the closest release distance (2.5 cm), several frequencies are detected (Figure 7 and 9). In addition to the fundamental frequency (1 Hz), the first and second harmonics are observed (2 Hz and 3 Hz). Only the fundamental frequency and first harmonic are detectable at the next closest release distance (5 cm). At even greater distances only the fundamental frequency is detectable. At the close distances, there is little mixing and diffusion of the packets before they are detected by the array. The sharp distinct edges of packets and their non sinusoidal nature cause the appearance of the harmonics.

3.3.4 Demonstrating Contact Senor Array Detection of an Object Modulated Plume

When a cylinder was used to modulate the plume (Figure 14 inset), wake around the cylinder causes increased lateral mixing and the plume width spans the entire linear sensor array. Therefore, the total averaged coherence spectra were calculated using all possible sensor pairs (Figure 14).

The detected modulation frequencies increase as the flow velocity increases and the observed and theoretical values are similar. For the 4 and 5 cm/s isokinetic release from the larger diameter release nozzle, the observed modulation frequency is slightly higher than the calculated shedding frequency. While a peak at the modulation

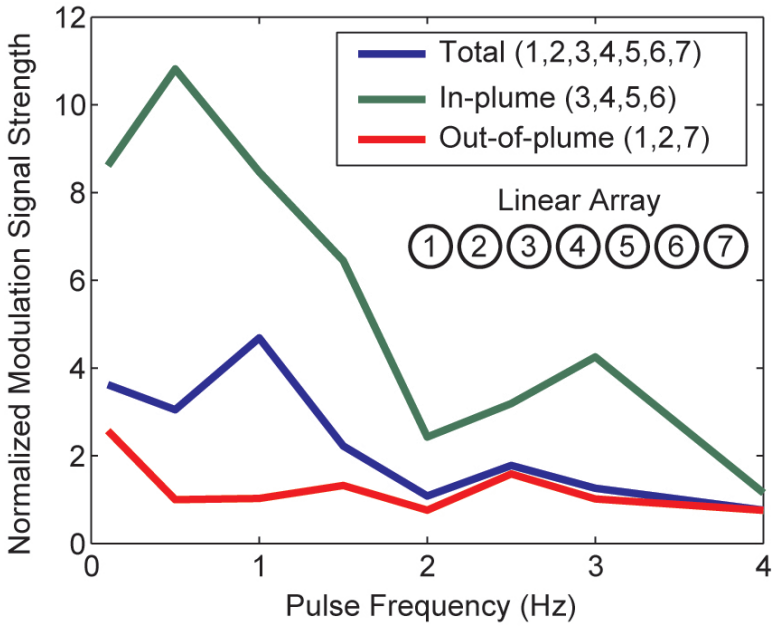

Figure 10: Coherence analysis of a linear contact array varying the pulse frequency: A solenoid valve was used to deliver a modulated plume at varying pulse frequencies to a linear sensor array (seven sensors 5 mm spacing) with a 5 cm release distance (Figure 4a). Time series were collected at each pulse frequency for 300 s and averaged coherence spectra for various sensor selections were calculated (Figure 6). Normalized modulation signal strength was calculated by dividing the coherence peak at the modulation frequency by the spectrum's baseline.

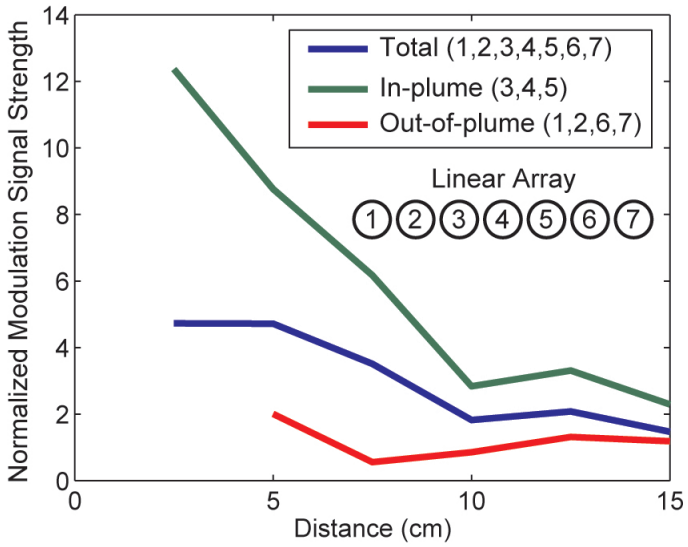

Figure 11: Distance information obtained from the coherence analysis of a linear contact array: A solenoid valve was used to deliver a modulated plume (1 Hz) to a linear sensor array (seven sensors 5 mm spacing) with varying release distances (Figure 4a). Time series were collected at each pulse frequency for 300 s, and averaged coherence spectra for various sensor selections were calculated (Figure 7). Normalized modulation signal strength was calculated by dividing the coherence peak at the modulation frequency by the spectrum's baseline.

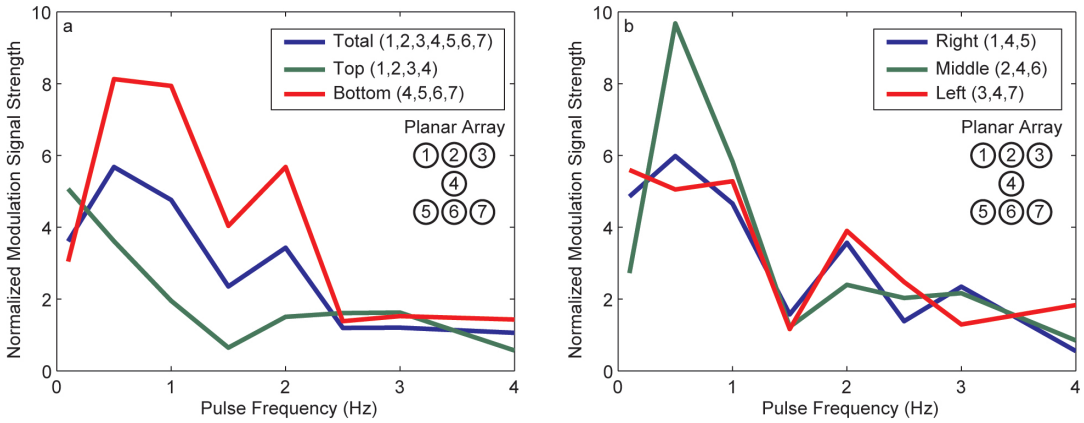

Figure 12: Coherence analysis of a planar array varying the pulse frequency: A solenoid valve was used to deliver a modulated plume at varying pulse frequencies to a planar sensor array (seven sensors 5 mm spacing) with a 5 cm release distance (Figure 4b). Time series were collected at each pulse frequency for 300 s, and averaged coherence spectra for various sensor selections were calculated (Figure 8). Normalized modulation signal strength was calculated by dividing the coherence peak at the modulation frequency by the spectrum's baseline. Effects from varying sensor selections by depth position (a) and lateral position (b) were observed.

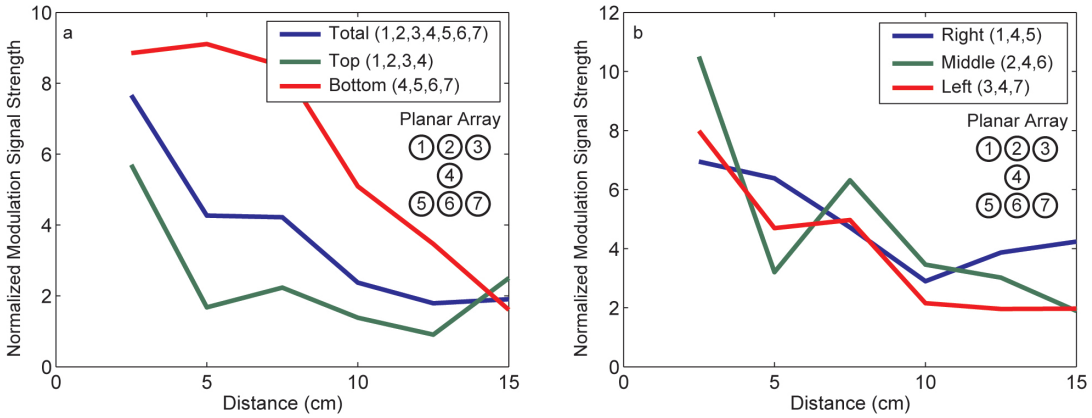

Figure 13: Coherence analysis of a planar array varying the release distance: A solenoid valve was used to deliver a modulated plume (1 Hz) to a planar sensor array (seven sensors 5 mm spacing) at varying release distances (Figure 4b). Time series were collected at each pulse frequency for 300 s and averaged coherence spectra for various sensor selections were calculated (Figure 9). Normalized modulation signal strength was calculated by dividing the coherence peak at the modulation frequency by the spectrum's baseline. Effects from varying sensor selections by depth position (a) and lateral position (b) were observed.

frequency is detectable, the peak is quite small and broad indicating that turbulent mixing is disrupting modulated plume structure.

When a higher concentration of marker is released from a smaller nozzle in a jet, the marker solution impinges on the cylinder, and based on dye visualization, the resulting odor packets are much more discrete. Additionally, lowering the free stream velocity decreases turbulent mixing. These methods were employed on the 3 cm/s flow velocity case and the expected 0.5 Hz signal was detectable (Table 1). For comparison, the 3 cm/s case was repeated without the cylinder for modulation; the unobstructed filament does not contain any specific frequency signal.

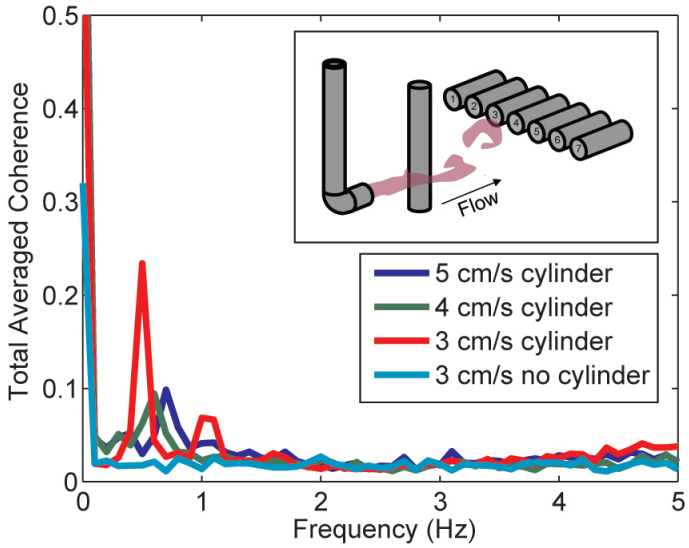

Figure 14: Effect of flow velocity on the coherence analysis of a object modulated plume. A cylinder is placed 2.5 cm downstream from the release nozzle, and the array was placed 8 cm downstream from the nozzle. The array height was 10 cm off the flume floor (inset). For the 4 and 5 cm/s cases, 50 mM ascorbic acid was isokinetically released from a 4 mm i.d. nozzle. For the 3 cm/s case, 50 mM ascorbic acid was released at 10 cm/s from a 2 mm i.d. nozzle. As a control, experimental data were collected as in the 3 cm/s case with a continuous plume release without the cylinder. Modulation frequency followed the expected trend with changes in flow velocity.

Table 1: Effects of Flow Rate on Modulation Frequency Around a Cylinder

flow rate (cm/s)	release	calculated frequency (Hz)	observed frequency (Hz)
5	isokinetic	0.8	0.7
4	isokinetic	0.7	0.6
3	jet	0.5	0.5
3	jet (no cylinder)	none expected	none observed

CHAPTER IV

CONCLUSIONS

In this study we have investigated the decoding of a modulated plume with noncontact (PLIF) arrays and contacting sensing arrays. In both cases the coherence analysis provides information about plume characteristics. It reveals that useful information can be encoded and decoded from the frequency domain of the chemical signal in a turbulent plume. This work has demonstrated that detection of the modulation frequency can be used to determine in-plume and out-of-plume sensors and thereby detect the relative orientation of the array in plume. Tuning the coherence analysis of the array by selecting specific sets of sensors provides insight in the orientation of the array toward the modulated plume and increases the information content. Such selection of the contributing sensors could be implemented automatically, by observing the magnitude of the raw signal at each sensor. The sensors with low signal magnitude can be switched off by not including their response in the analysis.

This information coupled with the known flow direction could theoretically be implemented as a strategy to track the source of an upstream chemical release. However, in a turbulent aquatic environment the modulated plume maintains a discrete structure for a relatively short distance from the source ($\sim$8 cm). This may limit coherence analysis application in systems requiring tracking over longer distances.

Although these modulation signals persisted only short distances from the source of the plume, the modulated signal strength could be increased by having more sensors in the plume, a more discrete signal, or collecting data for longer periods of time. Reducing the flow rate to decrease turbulent mixing or increasing the marker solution concentration could improve packet discreteness. However, there would be limited

control over the flow environment in real world aquatic plume tracking such as finding chemical source in a river bed or ocean environment.

Further investigation of the correlation between periodic fluctuations and the optimal selection and configuration of sensors would lead to a better understanding of encoded frequencies in chemical signals. These results indicate that increasing the size of the sensor array could greatly increase the efficiency of correlation analysis. In principle, a cluster of closely spaced individual sensors can form an array to enhance the selectivity of chemical detection. Arranging such clusters into a superarray may enhance frequency and spatial information extraction. Animals have such close spacing and abundance of chemoreceptors. Another intriguing and unanswered question is whether aquatic animals also use some form of correlation analysis in their search strategies.

REFERENCES

[1] M. J. Weissburg, D. B. Dusenbery, H. Ishida, J. Janata, T. Keller, P. J. W. Roberts, and D. R. Webster. A Multidisciplinary Study of Spatial and Temporal Scales Containing Information in Turbulent Chemical Plume Tracking. *Environmental Fluid Mechanics*, 2:65–64, 2002.

[2] M Taillefert, GW Luther, and DB Nuzzio. The application of electrochemical tools for in situ measurements in aquatic systems. *ELECTROANALYSIS*, 12(6):401–412, APR 2000.

[3] NJ Vickers. Mechanisms of animal navigation in odor plumes. *BIOLOGICAL BULLETIN*, 198(2):203–212, APR 2000.

[4] H. Ishida, T. Nakamoto, T. Moriizumi, T. Kikas, and J. Janata. Plume-Tracking Robots: A New Application of Chemical Sensors. *Biological Bulletin*, 200:222–226, 2001.

[5] DR Webster, S Rahman, and LP Dasi. Laser-induced fluorescence measurements of a turbulent plume. *JOURNAL OF ENGINEERING MECHANICS-ASCE*, 129(10):1130–1137, OCT 2003.

[6] DR Webster, PJW Roberts, and L Ra'ad. Simultaneous DPTV/PLIF measurements of a turbulent jet. *EXPERIMENTS IN FLUIDS*, 30(1):65–72, JAN 2001.

[7] DR Webster and MJ Weissburg. Chemosensory guidance cues in a turbulent chemical odor plume. *LIMNOLOGY AND OCEANOGRAPHY*, 46(5):1034–1047, JUL 2001.

[8] PA MOORE and J ATEMA. SPATIAL INFORMATION IN THE 3-DIMENSIONAL FINE-STRUCTURE OF AN AQUATIC ODOR PLUME. *BIOLOGICAL BULLETIN*, 181(3):408–418, DEC 1991.

[9] J MURLIS, JS ELKINTON, and RT CARDE. ODOR PLUMES AND HOW INSECTS USE THEM. *ANNUAL REVIEW OF ENTOMOLOGY*, 37:505–532, 1992.

[10] T Yamanaka, H Ishida, T Nakamoto, and T Moriizumi. Analysis of gas sensor transient response by visualizing instantaneous gas concentration using smoke. *SENSORS AND ACTUATORS A-PHYSICAL*, 69(1):77–81, JUN 30 1998.

[11] CHK Williamson. Vortex dynamics in the cylinder wake. *ANNUAL REVIEW OF FLUID MECHANICS*, 28:477–539, 1996.

[12] M Ozgoren. Flow structure in the downstream of square and circular cylinders. *FLOW MEASUREMENT AND INSTRUMENTATION*, 17(4):225–235, AUG 2006.

[13] SC LUO, MG YAZDANI, YT CHEW, and TS LEE. EFFECTS OF INCIDENCE AND AFTERBODY SHAPE ON FLOW PAST BLUFF CYLINDERS. *JOURNAL OF WIND ENGINEERING AND INDUSTRIAL AERODYNAMICS*, 53(3):375–399, DEC 1994.

[14] B.D. Dickman, D.R. Webster, J. L. Page, and M.J. Weissburg. Three-dimensional odorant concentration measurements around actively tracking blue crabs. *LIMNOLOGY AND OCEANOGRAPHY*, 7:96–108, 2009.

[15] T Kikas, H Ishida, PJW Roberts, DR Webster, and J Janata. Virtual plume. *ELECTROANALYSIS*, 12(12):974–979, AUG 2000.

[16] T Kikas, H Ishida, and J Janata. Chemical plume tracking. 3. Ascorbic acid: A biologically relevant marker. *ANALYTICAL CHEMISTRY*, 74(15):3605–3610, AUG 1 2002.

[17] T Kikas, P Janata, H Ishida, and J Janata. Chemical plume tracking. 2. Multiple-frequency modulation. *ANALYTICAL CHEMISTRY*, 73(15):3669–3673, AUG 1 2001.

[18] T Kikas, H Ishida, DR Webster, and J Janata. Chemical plume tracking. 1. Chemical information encoding. *ANALYTICAL CHEMISTRY*, 73(15):3662–3668, AUG 1 2001.